Eur. Phys. J. B **54**, 217–223 (2006)
DOI: 10.1140/epjb/e2006-00444-x

THE EUROPEAN PHYSICAL JOURNAL B

Lateral carrier tunnelling in stacked In(Ga)As/GaAs quantum rings

W. Ouerghui[1,a], J. Martinez-Pastor[2], J. Gomis[2], M.A. Maaref[1], D. Granados[3], and J.M. García[3]

[1] Unité de Recherche Des Physiques des Semiconducteurs et Capteurs, Institut Préparatoire aux Études Scientifiques et Techniques, La Marsa 2070, Tunis, Tunisia
[2] Instituto de Ciencia de los Materials, Universidad de Valencia, P.O. Box 22085, 46071 Valencia, Spain
[3] Instituto de Microelectrónica de Madrid, Isaac Newton 8, 28760 Tres Cantos, Madrid, Spain

Received 21 June 2006 / Received in final form 6 November 2006
Published online 22 December 2006 – © EDP Sciences, Società Italiana di Fisica, Springer-Verlag 2006

Abstract. Exciton recombination dynamics in vertical stacks of InGaAs quantum rings have been studied by means of continuous wave and time resolved photoluminescence under low excitation density conditions. We have paid special attention to the effect of the carrier coupling on the exciton radiative lifetime: weak (14 nm spacer sample), intermediate (4.5 nm spacer sample), where the size filtering effects (towards small rings) compensate partially that arising from carrier coupling (towards lower energies), and strong electron and hole coupling (1.5 nm spacer sample) between layers. Experimental decay times in the latter two cases have been compared to the times simulated with a multi-quantum well based model, which accounts for the observed change of carrier coupling regime. The most important effect is observed when the hole wave function overlap along the growth direction becomes important (1.5 nm spacer sample). This situation makes important the lateral tunneling of excitons between rings, given their large lateral size, which is characterized by times around 5 ns at the emission peak energy (rings with the most probable size of the distribution).

PACS. 71.55.Eq III-V semiconductors – 73.43.Jn Tunneling – 73.21.Ac Multilayers – 71.35.-y Excitons and related phenomena

1 Introduction

The interest in quantum dot (QD) based structures are growing in the last years [1–8]. Several semiconductor devices have been yet studied, as laser diodes and cascade lasers, photo detectors and emitters operating at mid-infrared wavelengths [9,10]. For these kind of devices multilayer stacks of QD is the most adequate architecture, due to the increase of the optical density of the active medium. It is well-known that the modal gain achieved in QD lasers increase proportionally to the number of stacked layers, which is not the case of the optical mode loss [11]. An additional benefit of stacking QD layers is their vertical correlation [12] and even a subsequent in-plane ordering of the nanostructures [13], due to the superposition of the strain fields coming from dots at the different layers. Moreover, the thickness of the barrier material deposited between QD (or quantum wires) layers can introduce changes in the emission wavelength by size filtering [14,15] and electronic coupling [16].

On the other hand, size and shape of the QD can be changed by using new strategies during the growth of a QD layer, like the overgrowth of the dots with a thin GaAs layer, as recently demonstrated [17]. Following this method, quantum rings (QR) can be obtained, which have interesting optical and magneto-optical properties [18]. Although the first QR were grown and studied some years ago, only a few research works have been reported up to now, as compared to typical QD. Particularly, QR ensembles are potential candidates for the development of lasers diodes at 980 nm at room temperature and high-speed optoelectronic devices. Stacked layers of QR have been grown for different GaAs spacers, demonstrating the laser operation in the most favourable cases [19]. The QR system allows a great density of multilayer stacks, because of their reduced height, more than three times smaller than typical QD, while avoiding excessive electronic coupling.

In this work we develop a complete optical study (continuous wave and time resolved photoluminescence) of QR shaped nanostructures stacked into a three layer structure exhibiting weak (14 nm GaAs spacer), moderate (4.5 nm GaAs spacer) and strong electron coupling (1.5 nm GaAs spacer). In principle, a certain degree of carrier wave function coupling along the vertical direction, and even in the plane, can contribute to increase the single-mode output power of laser diodes based on QD stacks, as predicted

[a] e-mail: ouerghuiwalid@yahoo.fr

by the model of Shi and Xie [20]. Such a situation is possible in a QR system, given the large in-plane dimensions. At the same time, many QR layers can be piled up along the growth direction, because the average heights of the QRs are typically below 1.5 nm. It allows the use of very narrow GaAs spacer layers to produce a certain degree of carrier coupling. In fact, we demonstrate in this work that a GaAs spacer as thin as 4.5 nm induces a relatively important electron wave function coupling along the vertical direction, but it does not change appreciably the exciton dynamics. This situation mainly produces a size (height) filtering effect of the stacked rings. In the limit of a very thin spacer, 1.5 nm, the electron coupling is very strong (the electron is practically delocalized over the three stacked QR layers) and recombination dynamics is affected by the lateral tunnelling of carriers between QR, as will be explained below in the framework of the bimodal QR size distribution existing in (each layer of) the studied samples.

2 Samples and experiment

The samples under study have been grown by molecular beam epitaxy (MBE). The QRs were obtained after a growth interruption when the dots were partially covered with 2 nm of GaAs under a flux of As_2, because of a balance between InGaAs alloying and InAs dewetting processes [21]. More details about the growth of this kind of samples can be found in references [19,22]. The three samples studied here contain three layers of QR stacked by using different GaAs spacer thickness: 14 (sample A), 4.5 (sample B) and 1.5 nm (sample C). In each layer, the total amount of deposited InAs was just above the critical thickness (1.6 ML) necessary for the 3D transition to take place, which induces low in-plane densities of nanostructures. The typical size of the original dots was around 20–40 nm diameter and around 11 nm of height, in average. The presence of QR nanostructures in these stacks have been revealed and studied by Atomic Force Microscopy (AFM), Transmission Electron Microscopy (TEM) [22] and Scanning Tunnelling Microscopy (STM) [23]. From AFM, typical dimensions obtained for QR are 100 nm $\times$ 90 nm $\times$ 1.5 nm. From TEM and STM, more morphological and compositional information is obtained for QR. In particular, the QR has not a homogeneous composition, as expected from its formation process, in which 2 nm of GaAs is used to partially cap the seed pyramidal dots. In this way, the central part of the ring, around 20 nm in diameter, is pure InAs, whereas the outer zone of the ring (up to the 100 nm of diameter typically measured by AFM) have a variable compositional profile of InGaAs due to the initial alloying effect of the original InAs dot and the 2 nm thick GaAs capping layer [22,23].

The continuous wave PL experiments were performed by using the 514 nm Ar^+line as excitation source. The PL signal was dispersed by a single 0.5 m focal length monochromatic and synchronously detected with a cooled Ge detector. In time resolved experiments, sample excitation at 750 nm was done by a green-ND:YVO_4 (Verdi, coherent) pumped mode locked Ti: Saphire laser (Mira 900D, coherent), providing 2 ps pulses at a repetition rate of 76 MHz. The PL signal was dispersed by a single 0.5 m focal length imaging spectrograph and detected by a synch Oscan streak camera (Hamamatsu C5680) with a type S1 cooled photocathode. The overall time response of the system in the widest temporal window (about 2 ns) was around 40 ps (full width at half maximum). In both kinds of experiments, the samples were held in the cold finger of a closed-cycle cryostat to vary the temperature in the range 12–300 K, approximately.

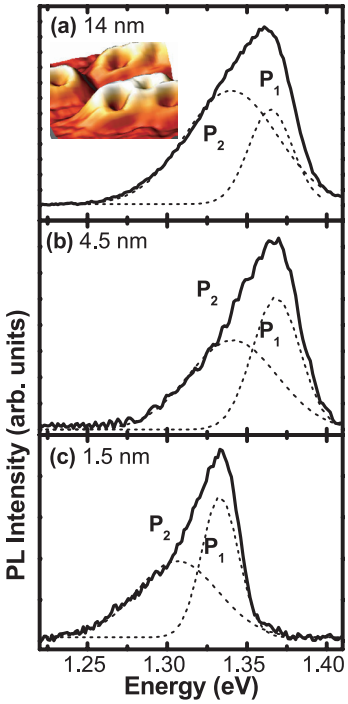

Fig. 1. PL spectra (continuous line) of samples A (a), B (b) and C (c) at 10 K. The excitation density was about 3 W/cm^2 at 514.5 nm. Dashed lines stand for the two-Gaussian deconvolution of the measured PL band.

3 Results and discussion

Figure 1 shows the low excitation density PL spectra (continuous lines) under non resonant excitation (514 nm) conditions, which are mainly dominated by exciton recombination at the ground states of the QR ensembles in the three samples with different GaAs spacer thickness (a to c spectra in Fig. 1). Their PL spectra are not perfect Gaussians, but rather asymmetric on their low energy side, independently of the GaAs spacer, as observed by comparing PL spectra in Figures 1a to 1c. Indeed, they can be reasonably deconvoluted into two Gaussian components, as shown in Figure 1 (dashed curves), which are separated by around 23–27 meV. The parameters of these Gaussian components, labelled as P1 (high energy component) and

Table 1. Gaussian parameters from the deconvolution of the PL spectra in Figure 1.

Sample id		Peak energy (eV)	FWHM (meV)	Intensity ratio P2/P1
A	P1	1.365	32	
	P2	1.340	68	2.5
B	P1	1.369	33	
	P2	1.342	60	1.3
C	P1	1.331	27	
	P2	1.308	60	1.2

P2 (low energy component), are listed in Table 1. We can see how the optical quality of these samples is rather good, because the high energy PL Gaussians have a line width narrower than 33 meV and dominate in their corresponding PL bands (mainly in samples B and C). Indeed, the line width of P1 is particularly narrow, 27 meV, in the case of sample C (see Tab. 1), which is a measure of a slight increase of quality when decreasing the GaAs spacer between the QR layers from sample A to C.

First of all, the two observed PL Gaussian components cannot be due to the contribution of excited states of a mono-modal QR size distribution; because when we use higher excitation densities we can perfectly observe that contribution (p-like exciton recombination) on the high energy side of the PL spectra. We attribute the measured PL band to a bi-modal size distribution of the QR ensemble (i.e., two different size families), being similar in each of the three stacked layers, in average. The measured energy separation between the two QR families, 23–27 meV, is approximately consistent with an average height fluctuation of 0.3 nm (one monolayer) [3,7,24]. We cannot attribute such two QR families to a different (mono-modal) size distribution in each one of the three stacked layers, because we would observe important changes in the PL band shape when reducing the GaAs spacer due to carrier wave function coupling. It would induce a different energy shift for smaller and bigger QR and hence the energy separation of PL Gaussian components would increase. In fact, the energy splitting between the electron levels of a structure containing three quantum wells (QW) of InAs (1 nm wide) separated by GaAs barriers 4.5 and 1.5 nm thick is expected to be around 29 and 127 meV, respectively, with respect to GaAs spacers thicker than 14 nm, after our estimate based on a transfer matrix method for InAs/GaAs QW systems [25]. The fact that the whole band (that measured in sample A) is shifted to the red more or less rigidly (the PL band does not change of shape) from sample A to C is a signature that the PL band is characteristic of the (same) QR size distribution in each layer of the stack, as assumed above.

Other than the origin of the measured asymmetric PL band, we must also discuss the effect of the vertical carrier wave function coupling produced by reducing the GaAs spacer thickness from sample A to C. Given the small height of the QR we only expect this coupling to be very important for electrons in samples B and C, due to the shallowness of their electron levels, and even for holes in the case of sample C. Our quantum well based simulation predicts a redshift of about 31 meV (this value is close similar for QD stacks with a comparable GaAs spacer thickness [26]) and 155 meV in the band-to-band optical transitions for samples B (4.5 nm spacer) and C (1.5 nm spacer), respectively, with respect to sample A (negligible coupling). These values would apply if any change in the size of the QR (QW thickness in our simulation) took place when stacking several layers separated by thin GaAs spacers. However, we can observe from Figure 1 and Table 1 that any appreciable redshift is measured between samples A and B and only a redshift of around 34 meV (38 meV) is measured in sample C with respect to sample A (B). Such differences between the expected and measured optical transition energies in QD stacks have been often reported in the literature, and attributed to changes in the overall size of the nanostructures being stacked [26]. That is, when reducing the GaAs spacer thickness, the average height of the stacked QD is somehow filtered towards smaller values, giving rise to significant blue energy shifts [14]. This can be the case when moving from sample A to B (PL slightly blueshifted by 4 meV), because we observe simultaneously a reduction of the ratio P2/P1 by a factor 2, approximately, that is, a reduction of big-QR density with respect to the original size distribution (that represented by sample A). When using an extremely narrow GaAs spacer, i.e. the case of sample C, the electronic coupling is so important that dominates over the size filtering effect. It is interesting to note that the average height of uncovered rings is around 1.5 nm, that is, very close to the used spacer thickness.

However, it is not expected to distinguish these possible big nanostructures from stacked QR giving rise to the low energy PL-Gaussian component, because of the extremely important electronic coupling. It will produce excitons practically delocalized over the three stacked QR layers and hence a situation close similar to an exciton confined in a single nanostructure three times high, as will be shown below within our multi-QW estimate.

Figure 2 shows the PL spectra (a) under resonant (dashed line) and non resonant (continuous line) excitation conditions and PLE spectra (b) detected at P2 (dashed line) and P1 (continuous line). Resonant excitation enables the two components of the PL band, P1 and P2, to be nicely resolved, mainly because the line width of P2 reduces now from 60 to 29 meV. At the same time, P1 and P2 are now at around 1.319 eV and 1.278 eV, slightly more shifted towards the red (12 and 30 meV for P1 and P2, respectively) than the same components measured under non resonant excitation, as observed in Figure 2a. Resonant PL spectra cannot be measured on samples A and B under similar conditions used to measure sample C, in spite of the strongly delocalized carrier wave function along the vertical direction. It can reflect the higher density of states in this situation, as compared to single QR layer. The PLE spectra detecting at the peak energies of components P1 (continuous line) and P2 (dashed line) in sample C are very different, as shown in Figure 2b. The PLE spectrum detecting at P1 exhibits

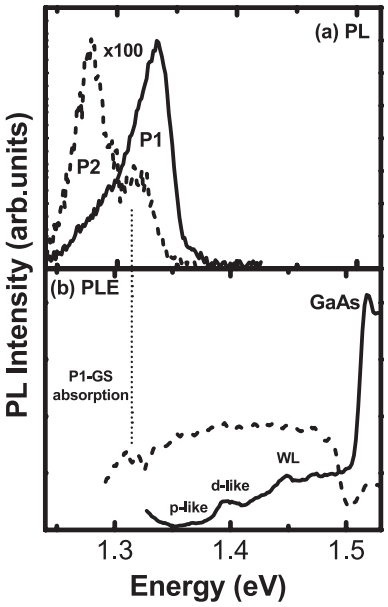

Fig. 2. (a) PL spectra under resonant (dashed line) and non-resonant (continuous line) excitation conditions in sample C; (b) PLE spectra detected at P2 (dashed line) and P1 (continuous line).

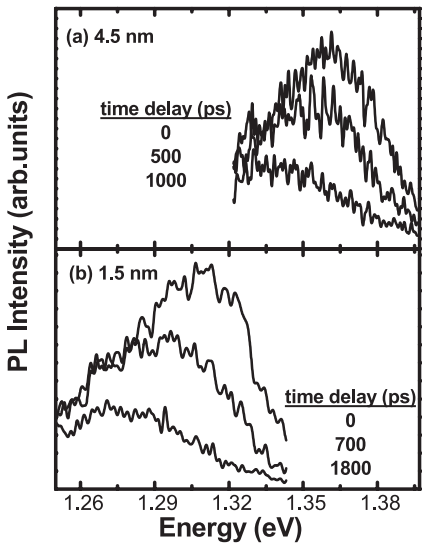

Fig. 3. Low temperature PL spectra for samples B (a) and C (b) at different delay times.

resonances at around 40 meV and 80 meV above the detection energy, which can be attributed to the absorption by p-and d-like excited state excitons of the P1-QR family, just like in usual single layer samples [27]. It is worth noting that these states arise from the lateral potential profile of QR [27], and hence they are less affected by the vertical coupling, especially for the smallest QR contributing to P1. The resonance at 1.449 eV can be associated with the absorption at the WL. At around 1.52 eV we observe the most intense resonance due to the GaAs exciton and direct band gap absorption. On the contrary, when the detection energy is chosen at P2 a minimum of PL intensity is detected at the GaAs absorption edge, which indicates a stronger capture probability by P1-rings as compared to P2-nanostructures, even if the latter are characterized by the lowest energy levels. At the same time, a practically structure less spectrum is measured below the GaAs absorption edge, except a broad resonance at around the peak energy of the P1 component. Somehow smooth resonances are also observed at around the energies of the expected p- and d-like exciton excited states of P1-rings and WL. Carrier tunneling from P1-rings toward the P2-nanostructures can be partly the origin of the strong PL signal measured in the P2-detected PLE spectrum. Additionally, the concurrence of a broader size distribution (the line width of P2-component was 60 meV), in which near QD-structures (non developed QR) could be also present [22], and vertically In(Ga)As alloyed nanostructures due to the thin GaAs spacer, as the most reliable possibilities, can be responsible of that structure less PLE spectrum. The hypothesis of a connection between states of P1-rings and P2-nanostructures is confirmed by results in Figure 3, in which the PL spectra for samples B (a) and C (b) are plotted for different delay times. We see how the PL is dominated by the P1-component at short times and by the P2-component at long times, which is especially evident for sample C. We will see below that the detection energy dependence of the exciton decay time cannot explain the observed red shift of the PL band with the delay time shown in Figure 3.

The above given picture is consistent with the TRPL results. We measure mono-exponential PL transients in the whole emission band of samples A, B and C, as representatively plotted in Figure 4 for the PL transients (dotted lines) registered at around the P1 peak energy. The continuous lines in Figure 4 represent the best exponential fits. The decay time measured in the case of sample C is appreciably lower than the values deduced in the other two samples, which are close similar. We can assume that "lateral" tunneling of carriers out of the P1-rings toward other rings of the size distribution with lower confined levels (QR giving rise to the low energy side of the P1-Gaussian component and, evidently, P2-nanostructures) can be the origin of the smaller value of the decay time measured at P1 energies in sample C, as suggested in the precedent paragraph. In other words, the measured decay time for P1-rings in sample C can be the combination of radiative and tunneling processes: $1/\tau_D = 1/\tau_R + 1/\tau_T$. The question arising now is why the tunneling out of the P1-rings is mainly observed for sample C and not for sample B (or A), if that "lateral" tunneling of carriers should be due to a high areal density of QR in each layer, which cannot be very different in all samples [22]. We can attribute the lateral tunnel in sample C to two reasons. Firstly, we can imagine that the three QR layers can be accounted for by multiplying also by three the tunneling probability. Secondly, the particles to tunnel laterally out of the QR must be excitons, because the electrons are strongly delocalized along the vertical direction in both samples B and C. That is, the vertical coupling of the hole wave function

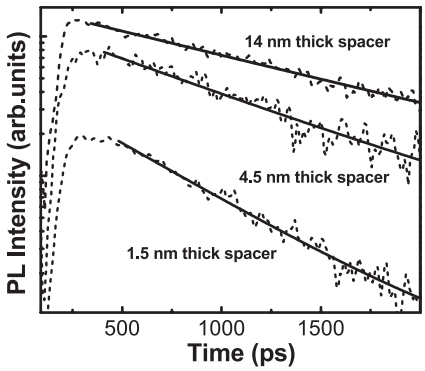

Fig. 4. Experimental PL transients at 10 K (dashed lines) registered at the P1 peak energy under low excitation density conditions (around 4 W/cm^2) for samples A, B and C and their corresponding mono-exponential fits (continuous lines).

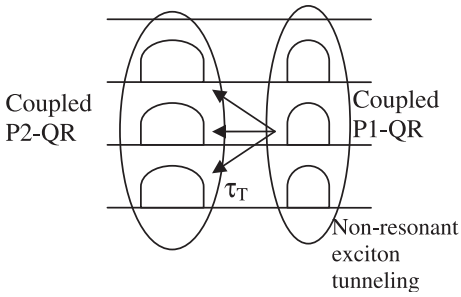

Fig. 5. Scheme of the non-resonant tunneling mechanism between QR of different average size.

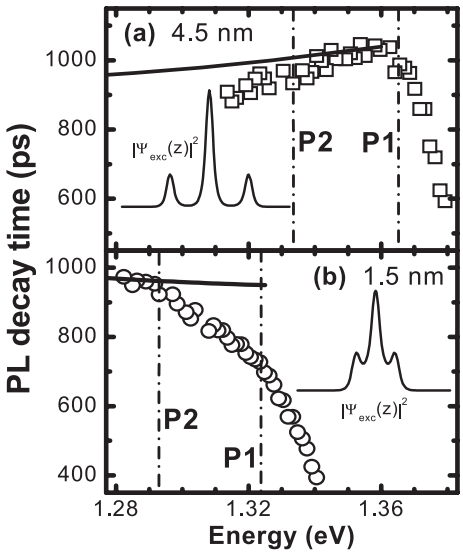

Fig. 6. Experimental decay time as a function of the detection energy for sample B, squares in (a), and C, circles in (b). Continuous lines represent our multi-QW simulation, as explained in the text. As insets in this figure we represent the characteristic electron-hole overlap function along the vertical direction for 4.5 (a) and 1.5 (b) nm thick GaAs barriers, within that simulation.

is determining most of the difference between samples B and C, from the point of view of the observed recombination dynamics. In fact, the electrons are affected by the coupling between the stacked QRs for layer separations of the order of 4.5 and 14 nm (samples B and A); while the heavy holes are affected by the coupling only for smaller GaAs thickness (1.5 nm in sample C). The situation is depicted in Figure 5, where the probability of non-resonant exciton tunneling is three times greater than that in a single layer, because the S-exciton at P1-QR can tunnel towards (near)P-states at P2-QR in every of the three layers.

Figure 6 shows the decay times measured on the whole PL band for samples B and C. The variation of the decay time as a function of the detection energy measured for sample B, which is shown in Figure 6a, is very similar to that in sample A, except the low energy region (below P1). Given the greater contribution of the P2 component to the PL band for sample A, as was shown in Figure 1a, and the size filtering effect induced by the use of thinner GaAs spacers (and possibly some more important alloying effect along the vertical direction) in samples B and C, we do not use here the time decays in sample A to discuss the observed different behaviour between samples B and C, which are more similar in morphological (size filtering and alloying effects) and optical (ratio P2/P1) aspects.

We can distinguish in Figure 6 two regions of interest. In the first region, below the P1 peak energy, we observe a different behaviour for samples B and C. We observe τ_D to increase with increasing detection energy for sample B, whereas it decreases for sample A. This first region must be attributed to the ground state oscillator strength variation with the dot size (determined by the size distribution), but influenced by the electron-hole coupling along the vertical direction. In the second region, above the P1 peak energy, we observe τ_D to decrease fastly with increasing detection energy in both samples. This second region can attributed to a more important contribution of exciton radiative recombination at excited states [28]. The s–p energy separation was only around 40 meV and detection above 1.36 (1.32) eV in sample B (C) can have the contribution of ground state recombination at P1-rings (those contributing to the high energy side of its PL component), but also that of excited state recombination at P2-rings (also bigger rings belonging to the P1 size distribution can participate above P1 peak energies).

Now we will concentrate on the first and more important region of detection energies, that below P1 peak. The most striking result was the different behaviour of the time decay dependence with detection energy: τ_D increases from 900 to 1050 ps for sample B and decreases from 1000 to 750 ps for sample C, as shown in Figure 6. The observed variation in sample B can be explained by the strong overlap of the electron envelop wave function, which will be more important for the smaller nanostructures of the distribution. At the same time, the coupling for heavy holes is still very weak to change appreciably with the size (height, mainly) and the electron-hole superposition is determined by the electron wave function. This behaviour is just that described by our multi-QW

simulation, which gives us an energy dependence of τ_R represented by the continuous line in Figure 6a. We have calculated electron and hole eigenfunctions, χ_e and χ_h, as a function of the well width (giving rise to band-to-band transition energies close to the experimental ones), which are separated by barriers 4.5 nm thick, and estimated the exciton radiative recombination time to be determined by the electron-hole overlap, $1/\tau_R = 1/\tau_0 \, |\langle \chi_e \mid \chi_h \rangle|^2$, where τ_0 is a time constant to compare with the experimental results. For a better comparison we represent the calculated recombination time as a function of the band-to-band optical transition (emission energy for experimental values).

The representative electron-hole overlap function (the exciton wave function probability along the vertical direction is proportional to it) is represented as an inset in Figure 6a. This multi-QW estimate is not very far from experimental results, which means that the exciton dynamics mainly arises from the height variation of the QR nanostructures. This is not the case of the same estimate performed for InAs wells separated by 1.5 nm thick GaAs barriers, represented by a continuous line in Figure 6b. Now, the simulated curve is far from the experimental decay time as a function of the PL detection energy measured in sample C. In any case, it is worth noting the fact that the change from negative to positive slope of $\tau_D(E_{PL})$ is perfectly reproduced by our simple estimate of $\tau_R(E_{PL})$, after reducing the barrier thickness between InAs layers (namely the GaAs spacer from sample B to C). That is, when the thickness of the GaAs spacer is 1.5 nm, the coupling for holes begins to be important and the electron-hole overlap takes place over the three wells, as illustrated in the inset of Figure 6b. Moreover, this overlap will be greater when decreasing the vertical size of the nanostructure (well width in our simulation), i.e., when increasing the PL detection energy. However, the decrease of the calculated $\tau_R(E_{PL})$ is very smooth as compared to the experimental $\tau_D(E_{PL})$ in sample C. Given the good agreement in the case of sample B, we can assume again that the difference between calculated $\tau_R(E_{PL})$ ant the experimental $\tau_D(E_{PL})$ is mainly due to the lateral tunneling of excitons (mainly determined by holes) out of the QR. This mechanism will be more important for carriers occupying excited states and ground state of the smaller QR of the size distribution (high energy tail of the PL band, above P1 peak). This is why we have assumed that τ_R should have approximately the value of the measured τ_D at the lowest PL detection energies (around P2 peak) in sample C. Figure 7 shows the obtained energy dependence of τ_T within the PL band in sample C, from P2 to slightly above P1 peak energy. We have calculated τ_T by means of the relation $1/(\tau_T(REAL)) = 1/3 \times [1/\tau_D(C) - 1/\tau_R(C)]$, which includes the increase of the tunneling probability by a factor 3 due to the three "coupled" QR layers, as was illustrated in Figure 5. We have performed two types of estimates, one more experimental (hollow symbols in Fig. 7), by assuming $\tau_R(C) = \tau_D(B)$ and doing a rigid energy shift of the experimental curve $\tau_D(C)$ (strongly redshifted by the coupling) in order to match P1 peak energy in both samples. A second estimate of τ_T (solid symbols in Fig. 7) has been performed by assuming $\tau_R(C)$ to be the calculated values from our multi-QW. In the latter case the same energy shift (40 meV) have been done to compare both types of results. They do not differ appreciably, which makes us confident about the quantitative order of magnitude obtained for the energy dependence of τ_T. At energies above P1 peak, dominated by excited state recombination, the value of τ_T tends to 5 ns, and grows near linearly by about 8 ns when decreasing PL detection energy from P1 to P2 (increasing the size of the QR). Values around 1 and 5 ns have been reported for non-resonant electron tunneling in vertically stacked dots separated 10 and 16 nm, respectively [29,30]. In the second case, the tunneling is only observed at high temperatures and hence attributed to a multiphonon-assisted tunneling mechanism. For lateral carrier tunneling we find the results reported in reference [31], where a value of around 3.5 ns is found for "carrier transfer" (excitons, after our opinion) in high density QD arrays from small dots emitting at around 1.3 eV towards bigger dots emitting at lower energies. This finding would be consistent with our results, even if it is not the same kind of ensemble. The measured average distance between QR is around 120 nm, which is of the order of the In(Ga)As ring diameter, as determined by AFM [22], and the QR ground states are only 90–110 meV (for P1-P2 families, respectively), comparable to the case of QD ensemble in reference [30]. The lateral coupling of nanostructures can be also a factor to take into account for laser diode engineering, as suggested in reference [19] to improve the single-mode operation, or to control the population of a given family of nanostructures in multimodal size ensembles, as suggested in reference [30].

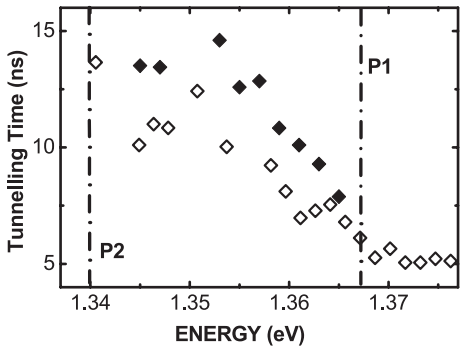

Fig. 7. Energy dependence of τ_T within the PL band in sample C, from P2 to slightly above P1 peak energy, under two assumptions: $\tau_R(C) = \tau_D(B)$ (hollow symbols), and $\tau_R(C)$ to be the multi-quantum well estimate shown in Figure 5b (solid symbols).

4 Conclusions

In this paper we have studied stacked InGaAs quantum ring layers, separated by thin GaAs barriers, by means of steady state and time resolved photoluminescence under very low excitation density conditions. We

have demonstrated how the strong electron and hole coupling between layers in the sample with 1.5 nm thick spacer is responsible of the lateral tunneling of excitons (being limited this mechanism by the heaviest particle) from the smaller rings of the ensemble (represented by family P1) towards the biggest ones (represented by family P2). The experimental results in samples B (strong electron coupling) and C (strong electron and hole coupling) have been compared to the radiative exciton lifetimes estimated by using a multi-quantum well based model, This model explains the change of slope of the measured $\tau_D(E_{PL})$ when passing from weak to relatively strong hole coupling, which is accentuated in sample C by the important contribution of the in-plane tunneling between nanostructures. This mechanism is characterized by tunneling times around 5 ns at the P1 peak energy (rings with the most probable size of the distribution). Our results are of interest to improve the single-mode operation of laser diodes based on QR high density stacks, or to control the population of a given family of nanostructures in multimodal size ensembles.

This work was partially supported by Spanish MCyT Nanoself-II Project No. TEC2005-05781-C03, the SANDiE Network of excellence (Contract No. NMP4-CT-2004-500101) and the AECI Spain-Tunisia bilateral research action No. 2/04/R.

References

1. N.N. Ledenstov, V.A. Shchukin, M. Grundmann, N. Kirstaedter, J. Böhrer, O. Schmid, D. Bimberg, V.M. Ustinov, A.Yu. Egorov, A.E. Zhukov, P.S. Kop'ev, S.V. Zaitsev, N.Yu. Gordeev, Zh.I. Alferov, A.I. Borovkov, A.O. Kosogov, S.S. Rumvimov, P. Werner, U. Gösele, J. Heydenreich, Phys. Rev. B **54**, 8743 (1996)
2. Q. Xie, A. Madhukar, P. Chen, N.P. Kobayashi, Phys. Rev. Lett. **75**, 2542 (1995)
3. S. Taddei, M. Collocci, A. Vinattieri, P.G. Gucciardi, F. Bogani, S. Franchi, P. Frigeri, L. Lazzarini, G. Salviati, Phys. Stat. Solidi A **224**, 413 (2001)
4. R.J. Luyken, A. Lorke, M. Fricke, J.P. Kotthaus, G. Medeiros-Ribeiro, P.M. Petroff, Nanotechnology **10**, 14 (1996)
5. G.S. Solomon, J.A. Trezza, A.F. Marshal, J.S. Harris Jr, Phys. Rev. Lett. **76**, 952 (1996)
6. M. Collocci, A. Vinattieri, L. Lippi, F. Bogani, M. Rosat-Clot, S. Taddei, A. Bosachi, S. Franchi, P. Frigeri, Appl. Phys. Lett. **74**, 565 (1999)
7. S. Taddei, M. Collocci, A. Vinattieri, F. Bogani, S. Franchi, P. Frigeri, L. Lazzarini, G. Salviati, Phys. Rev. B **62**, 10220 (2000)
8. M.S. Miller, J.O. Malm, M.E. Pistol, S. Jeppesen, B. Kowalsi, K. Georgsson, L. Samuelson, J. Appl. Phys. **80**, 3360 (1996)
9. V.M. Apalkov, T. Chakraborty, Appl. Phys. Lett. **78**, 1820 (2001)
10. S. Sauvage, P. Boucaud, T. Brunhes, A. Lemaitre, J.M. Gerard, Phys. Rev. B **60**, 15589 (1999)
11. P.M. Smowton, E. Hermann, Y. Ning, H.D. Summers, P. Blood, Appl. Phys. Lett. **78**, 2629 (2001)
12. K. Eberl, O.G. Schmidt, R. Duschl, O. Kienzle, E. Ernst, Y. Rau, Thin Solid Films **369**, 33 (2000)
13. J. Tersoff, C. Teichert, M.G. Lagally, Phys. Rev. Lett. **76**, 1675 (1996)
14. J. Martínez-Pastor, B. Alén, C. Rudamas, Ph. Roussignol, J.M. García, L. González, Physica E **17**, 46 (2003)
15. B. Alen, J. Martinez-Pastor, J.M. Garcia, L. Gonzalez, A. Ponce, S.I. Molina, R. Garcia, Phys. Rev. B **65** R 241 301
16. S. Taddei, M. Colocci, A. Vinattieri, F. Bogani, S. Franchi, P. Frigeri, L. Lazzarini, G. Salviati, Phys. Rev. B **62**, 10220 (2000)
17. D. Granados, J.M. García, Appl. Phys. Lett. **82**, 2401 (2003)
18. R.J. Warburton, C. Schäflein, D. Haft, F. Bickel, A. Lorke, K. Karrai, J.M. Garcia, W. Schoenfeld, P.M. Petroff, Nature **405**, 926 (2000)
19. F. Suarez, D. Granados, M.L. Dotor, J.M. Garcia, Nanothechnology **15**, S126 (2004)
20. B. Shi, Y.H. Xie, Appl. Phys. Lett. **82**, 4788 (2003)
21. M.L. Dotor Recio, D. Golmayo, F. Briones, J. Appl. Phys. **72**, 5861 (1992)
22. D. Granados, J.M. García, T. Ben, S.I. Molina, Appl. Phys. Lett. **86**, 071918 (2005)
23. P. Offermans, P.M. Koenraad, J.H. Wolter, D. Granados, J.M. García, V.M. Fomin, V.M. Gladilin, J.T. Devreese, Appl. Phys. Lett. **87**, 131902 (2005)
24. W. Jaskolski, M. Zielinski, G.W. Bryant, Acta Physica Polonica A **106**, 193 (2004)
25. *The effective strained InAs band gap energy (778 meV), the energy barrier for electrons and holes (465 and 276 meV), respectively, and the electron and hole effective masses for InAs and GaAs are taken from:* O. Stier, M. Grundmann, D. Bimberg, Phys. Rev. **B** 59, 5688 (1999); *The algorithm for the one-dimensional TMM simulation has been taken from*: B. Jonsson, S.T. Eng, IEEE J. Quantum Electronics **26**, 2025 (1990)
26. M. De Giorgi, A. Taurino, A. Passaseo, M. Catalano, R. Cingolani, Pys. Rev. B **63**, 245302 (2001)
27. B. Alén, J. Martínez-Pastor, D. Granados, J.M. García, Phys. Rev. B **72**, 155331 (2005)
28. F. Adler, M. Geiger, A. Bauknecht, F. Scholz, H. Schweizer, M.H. Pilkuhn, B. Ohnesorge, A. Forchel, J. Appl. Phys. **80**, 4019 (1996)
29. A. Takeuchi, T. Kuroda, K. Mase, Y. Nakata, N. Yokoyama, Phys. Rev. B **62**, 1568 (2000)
30. Yu.I. Mazur, X. Wang, Z.M. Wang, G.J. Salamo, M. Xiao, H. Kissel, Appl. Phys. Lett. **81**, 2469 (2002)
31. J.W. Tomm, T. Elsaesser, Yu.I. Mazur, H. Kissel, G.G. Tarasov, Z.Ya. Zhuchenko, W.T. Masselink, Phys. Rev. B **67**, 04 5326 (2003)